Hindawi Publishing Corporation
Mathematical Problems in Engineering
Volume 2015, Article ID 921413, 11 pages
http://dx.doi.org/10.1155/2015/921413

Research Article

The Fracture Influence on the Energy Loss of Compressed Air Energy Storage in Hard Rock

Hehua Zhu,[1] Xingyu Chen,[1] Yongchang Cai,[1] Jianfeng Chen,[1] and Zhiliang Wang[2]

[1]*State Key Laboratory of Disaster Reduction in Civil Engineering, College of Civil Engineering, Tongji University, Shanghai 200092, China*
[2]*Department of Civil Engineering, Hefei University of Technology, Anhui 230009, China*

Correspondence should be addressed to Yongchang Cai; yccai@tongji.edu.cn

Received 15 March 2015; Revised 8 June 2015; Accepted 9 June 2015

Academic Editor: Timon Rabczuk

A coupled nonisothermal gas flow and geomechanical numerical modeling is conducted to study the influence of fractures (joints) on the complex thermohydromechanical (THM) performance of underground compressed air energy storage (CAES) in hard rock caverns. The air-filled chamber is modeled as porous media with high porosity, high permeability, and high thermal conductivity. The present analysis focuses on the CAES in hard rock caverns at relatively shallow depth, that is, ≤100 m, and the pressure in carven is significantly higher than ambient pore pressure. The influence of one discrete crack and multiple crackson energy loss analysis of cavern in hard rock media are carried out. Two conditions are considered during each storage and release cycle, namely, gas injection and production mass being equal and additional gas injection supplemented after each cycle. The influence of the crack location, the crack length, and the crack open width on the energy loss is studied.

1. Introduction

Large-scale energy storage is the key technique to solve the energy regulation and distribution for the future renewable energy development. It also contributes to the wider application and regulation applications of renewable energy being accessible to the utility grid. Compressed air energy storage (CAES) is an energy storage technique that converts electricity or heat to the potential energy by storing highly pressurized air in underground caves. The pressurized air is released and reconverted to electricity through gas turbines when needed [1] as shown in Figure 1. CAES is among the most efficient energy storage methods which is capable of meeting huge energy demand within a short period of responding time. Compared with hydropower stations, CAES is more economical and requires shorter construction period [2].

The storage of high pressure air in subsurface rock cavern brings new geological challenge to the site location. Suitable formation is not only to provide adequate cavity stability but also to meet the requirements of air tightness. Different location decisions have been proposed including salt rock caverns formed by dissolving, hard rock caverns, natural fractured porous aquifers, and the shallow buried caverns with lining [3, 4]. Salt rock caverns are formed by economical dissolving method and tend to be relatively homogeneous and dense [3]. To date, the only two CAES plants in operation at utility scales are all built in salt formation. The first one is the Huntorf plant in Germany built in 1978 and the second is the ACE plant built in McIntosh, in 1991 [5]. Caverns built in salt rock are generally high and narrow, such as the Huntorf and Mclntosh, which go against the stability of large caverns. Furthermore, the existence of weak interlayer restricts the scale of plants built in salt rock [6]. When CAES plants are built in porous aquifer, high pressure air displaces groundwater and gets balance with groundwater head during the process of air compressing. Then the gas pressure decreases and groundwater flows back during the process of air releasing. The adequate porous aquifers require impervious layer, enough water supply, sufficient permeability, and porosity. However, periodic large-scale groundwater seepage and complex groundwater chemical corrosion deteriorate the structure of the porous aquifer during the process of CAES plant operation [3]. CAES plants built in

hard rock could provide more air storage space but the cost of excavating new caverns in hard rock is very expensive (about $30 per kWh) [7]. The use of depleted mines of the oil and gas fields saves the cost of constructing underground space for gas storage. Subsurface hard rock can withstand higher pressure fluctuations than the salt rock which has a typical tensile strength of about 7-8 MPa. An appropriate site to build gas storage cavern in hard rock requires low permeability, good integrity, and less developed joint fissures to meet the requirements of air tightness [3].

As hard rock has better mechanical properties and is able to support higher gas pressure, plants built in hard rock formation have higher output power than those in salt rock. As a result, the research of utilizing hard rock is very important and in this paper we carried out the energy analysis of utilizing hard rock cavern for CAES through a coupled thermalhydromechanical modelling for physical quantities.

Numerical methods for the THM modelling have been advanced in the past few decades, especially in the application for geothermal energy exploitation and waste disposal [8]. Conventional methods for THM modelling are mainly based on continuum theory with focus of damage or smeared crack model [9]. The finite element method (FEM) is mostly used as the numerical discretization for the field variables. However, the crack energy release and crack kinematics cannot be correctly modeled in a damage or smeared crack model. Such type of method is commonly noted as "weak discontinuity." To remove the limit of "weak discontinuity," there have been growing interests of modelling propagating crack where the discontinuous displacement and stress concentration take place in the vicinity of crack, including the meshless methods [10, 11], phantom node method [12], edge rotation finite element method [13], extended isogeometric analysis [14, 15], and finite cover method [16, 17]. Multiscale methods [18, 19] have also been devised to study the interaction between different fields.

There are several advanced methods to model the fracture. In the cracking particles method [20, 21], the crack can be arbitrarily oriented and no representation of the crack topology is needed. The crack is modelled in three dimensions by a local enrichment of the test and trial functions with a sign function, so that the discontinuities of displacement across the crack can be captured. A coarse-graining technique [22] is proposed to reduce a given atomistic model into an equivalent coarse grained continuum model. The developed technique is tailored for problems of involving complex crack patterns in 2D and 3D including crack branching and coalescence. In the adaptive multiscale method [23], the phantom node method is used to model the crack in the continuum region and a molecular statics model is used near the crack tip. However, the method is only implemented in a two-dimensional code. A concurrent coupling scheme [24] is proposed to model three-dimensional cracks and dislocations at the atomistic level. Moreover, a method to couple a three-dimensional continuum domain to a molecular dynamics domain [25] for dynamic crack propagation is proposed. The continuum domain is treated by an extended finite element method to handle the discontinuities.

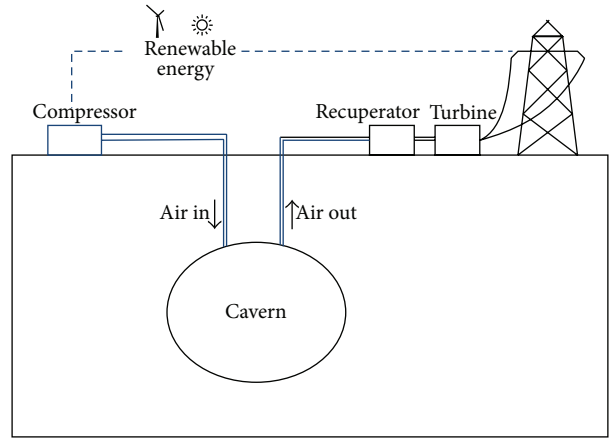

Figure 1: Compressed air energy storage plant.

2. THM Modelling for CASE

Since the 1980s, due to the deep resources exploitation, oil and gas field development, and nuclear waste storage, the coupled thermalhydromechanical modelling in rock became the focus of research. The basic coupled thermalhydromechanical equations in the saturated rock medium were proposed based on the extension of Biot consolidation theory in 1984 [26]. Based on continuum theory and pore elasticity theory, the coupling coefficients were studied quantitatively, and it was revealed that the influence of temperature on the stress field should not be neglected [27]. For unsaturated porous media, the THM coupling model and the finite element equations of the coupling problem were established based on the Galerkin method [28]. For the saturated-unsaturated media and fractured rock mass, systematic research on the coupling problem was conducted [29, 30].

The cavern of CASE plants is subjected to the coupled thermalhydromechanical (THM) effects. During the process of gas compressing and releasing, the temperature in cavern changes periodically and the heat is transferred from cavern to surrounding rock through thermal conduction and convection so that the thermal field of formation changes accordingly. As surrounding rock belongs to the porous medium, high pressure air seeps outside through joints and pores in the rock and changes the pore pressure field in rock strata. The change of temperature field and pore pressure also leads to the change of stress field in surrounding rock. Besides, the air has higher compressibility than liquid, which cannot be handled as incompressible fluid simply. The gas viscosity also changes with temperature and pressure. Furthermore, the CAES cavern suffers periodic THM coupling effects due to periodic air compressing and releasing in operation.

Given these features of the CAES cavern mentioned above, researches aimed at modelling the coupled THM process for CAES plant. Raju and Kumar Khaitan [31] deduced mass and energy balance equations for the gas storage cavern. They simulated the CAES plants operation and found that high pressure air and heat transfer between caverns and rocks had significant influence on the thermodynamics state of the air in cavern. However, the simulation assumed that

the rock temperature was constant and did not consider gas seepage into rock mass so as to restrict the application of the result. Kushnir et al. [32] studied parameters that affected the temperature and pressure fluctuations and the volume of gas storage. The heat transfer between the rock and air reduced the pressure and temperature fluctuations during the process of air compressing and releasing and increased effective energy storage capacity. They have also found that operating pressure ratio (maximum pressure\minimal pressure) was an important factor to decide gas storage volume. However, the study only focused on the gas thermodynamic status inside the cavern and did not involve the response of surrounding rock under the complicated coupled THM condition. Kim et al. [4] explored the possibility of the construction of CAES power station in lined shallow buried cavern. They analyzed the time and space distribution of gas seepage and energy loss in the cavern (100 meters in depth and diameter of 5 meters) employing TOUGH and FLAC. The permeability of concrete lining and surrounding rock was the main factor that influenced the tightness of gas storage in the short and long term. At the same time, energy loss due to heat transfer would be minimal if the injected air temperature was similar to the rock temperature. However, the study did not involve stress field and could not analyze the stability of caverns directly. Zhuang et al. [33] conducted coupled nonisothermal gas flow and geomechanical numerical modeling to study the complex thermohydromechanical (THM) performance of CAES built in hard rock. Governing equations were deducted from basic energy balance law, mass balance law, and the static equilibrium equation. They explored the THM coupling performance of cavern in intact rock media and in rock media with one discrete crack. However, the study did not involve multiple cracks. In this paper, we aim to figure out energy loss induced by the existence of multiple cracks and the influence of the crack location, the crack length, and the crack open width on the energy loss.

Table 1: Material parameters used in example.

Parameters	Value in cavern	Value in formation
Young's modulus E (GPa)	—	35
Poisson's ratio υ	—	0.3
Density (kg/m^3)	Determined by T and P	2800
Pore ratio ϕ	1.0	0.01
Permeability coefficient k (m^2)	1×10^{-9}	1×10^{-20}
Permeability coefficient along crack k_f (m^2)	—	1×10^{-17}
Crack width d_f (m)	—	0.1
Viscosity of air η (Pa·s)	1.86×10^{-5}	1.86×10^{-5}
Biot's consolidation coefficient b	0.95	0.95
Heat conduction of rock α_s (W/m·K)	3	3
Heat conduction of air α_s (W/m·K)	1000	0.56
Specific heat of air under constant pressure $C_{p,\text{gas}}$ (J/kg·K)	1000	1000
Specific heat of rock $C_{p,s}$ (J/kg·K)	900	900
Expansion coefficient β (1/K)	1.0×10^{-5}	1.0×10^{-5}
Initial pressure P_0 (atm)	1	1
Initial temperature T_0 (K)	286.15	286.15
Air injection temperature T_{in} (K)	296.65	—

3. Energy Analysis of the CAES System in Hard Rock

In this paper, the complete coupling model of mechanical, thermal, and hydro fields was employed. In this complete model, rock temperature fluctuation causes the rock volumetric strain and the rock strain leads to the change of rock deformation and fluid seepage. At the same time, porous media deformation and fluid seepage affect the temperature field. The seepage influences temperature field through the fluid convection while stress field affects temperature field through mechanical work and volume strain. As the temperature fluctuation is small in operation, the influence of temperature on the viscosity of the air was ignored. At the same time, we also did not consider the influence of temperature on the rock mass mechanics parameters. We adopted the assumptions and governing equations described in [33] to study the energy loss for CAES in subsurface hard rock.

The diameter of the underground cavern embedded with 100 m depth is 5 m. Table 1 shows the parameters employed in this case study. At the beginning, the air is injected at the rate of 1.12×10^{-3} kg/(s · m^3) for 16 hours to reach 5.5 MPa and stored for 8 hours to start daily circulation. In the stage of daily air compressing, the air at temperature of 296.65 K (23.5°C) is injected into the cavern at the rate of 1.12×10^{-3} kg/(s · m^3). In the energy recuperation stage, the air is released at the rate of 2.24×10^{-3} kg/(s · m^3).

According to the first law of thermodynamics, the change in total energy (Δ) stored in the CASE underground cavern can be expressed as the summation of the change in internal energy (ΔE), the work done by injected compressed air (ΔW), and the sum of outflows by production, air leakage, and heat transfer (ΔQ) [4]

$$\begin{aligned} \Delta &= \Delta E + \Delta W + \Delta Q, \\ \Delta E &= C_{\text{air}} \cdot T \cdot \Delta m, \\ \Delta W &= \Delta P \cdot V = R_{\text{air}} \cdot T \cdot \Delta m, \end{aligned} \tag{1}$$

where Δm (kg/s) is the air mass flow, C_{air} (J/kg · K) is the specific heat of air, T (K) is the temperature in cavern, P (Pa) is the pressure in cavern, and V (m^3) is volume of the cavern.

The total injected energy (E_{in}) consists of the internal energy of injected air and the work done during compression. The output energy (E_{out}) consists of the internal energy of released air and the work done during air releasing stage. The difference between injected energy and output energy is the energy loss (Q) caused by heat conduction, advection, and air leakage

$$E_{in} = (C_{air} + R_{air}) \cdot T \cdot m_{in},$$
$$E_{out} = \int_{t_1}^{t_2} (C_{air} + R_{air}) \cdot T_i \cdot m_{out} \cdot dt, \quad (2)$$
$$Q = E_{in} - E_{out},$$

where T (K) is the temperature of injected air, m_{in} (kg/s) is the injected rate of air, t (s) is the compression time, T_i (K) is the temperature of released air, m_{out} (kg/s) is the released rate of air, t_1 (s) is the start time of the air releasing stage, and t_2 (s) is the end time of the air releasing stage.

The study explored the energy loss analysis of the cavern in intact rock and in rock with multiple cracks. Without water concealing, supplementary air injection is necessary to maintain operational pressure due to air seepage [33]. Evaluation was carried out in two cases. Case one is with equal gas injection and production during each compression and decompression cycle, namely, the mass conservation control. Case two is with additional gas injection, namely, the air supplement control. With the mass conservation control, 189.1 MJ of energy was injected each day while 195.25 MJ of energy was injected each day with the air supplement control.

3.1. Energy Analysis in Rock with Single Crack. The energy output and energy loss in intact hard rock are shown in Figures 2 and 3. Due to the air leakage and with no supplement, the output energy declined over time with the mass conservation control, which did not conform to the industry requirements. Energy loss grew up quickly in the first 10 days and then the growth became slow. With the air supplement control, the output energy was more stable and higher than that with mass control. The difference was more and more significant over time, which proves that the supplementary air can guarantee stable output power of CAES plant in hard rock. Besides, the energy loss with air supplement control reached 12 MJ, which was higher than 7 MJ with mass control. Thermodynamic analysis showed that 3.4% of energy injected was lost to the surrounding media in intact rock in the 25th day with mass control while 6.14% of energy injected was lost in the 25th day with air supplement control. However, the energy loss with air supplement control remained stable over time but that with mass control grew continually.

To study the impact of single crack on energy loss, we set the crack width as 0.1 m and length as 9.5 m and the location is on the top of the carven. In hard rock with single crack, the changing trend was similar to that in intact rock as shown in Figures 4 and 5. With air supplement control, the CASE

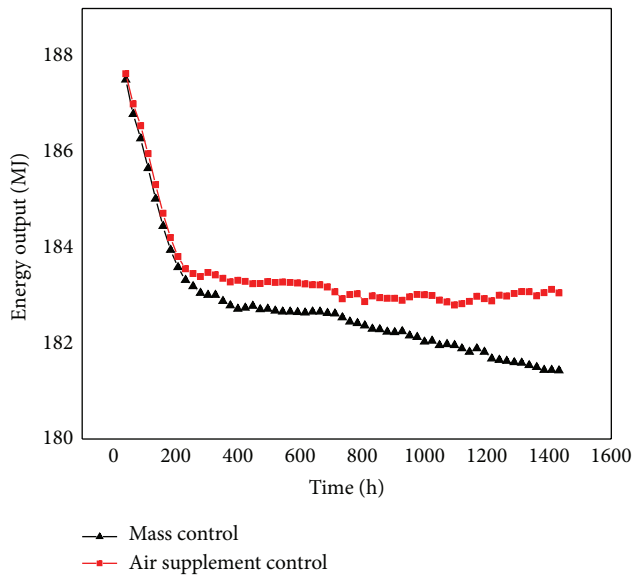

Figure 2: Energy output in intact hard rock.

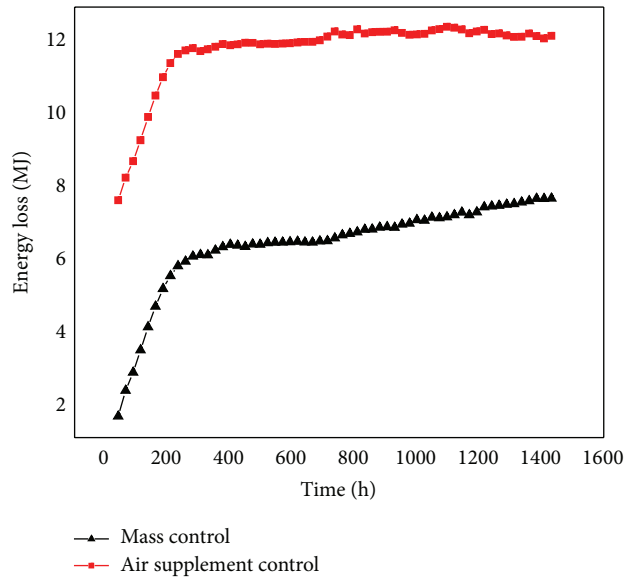

Figure 3: Energy loss in intact hard rock.

plant still had stable output energy and energy loss stood at 12 MJ in the long term. Due to the existence of crack, the output energy with mass control was considerably below that with air supplement control at the beginning and the gap expanded over time. For the hard rock with cracks, additional gas injection is a necessary method to ensure the normal operation of the plant at the expense of higher energy loss.

As shown in Tables 2 and 3, the efficiency comparison has been conducted in the 12th and 20th day. In intact rock, thermodynamic analysis showed that 3.41% of energy injected was lost to the surrounding rock in the 20th day with mass control while 6.14% of energy injected was lost with air supplement control. In rock with single crack, the efficiency reached 95.35% with mass control and 93.71% with

Table 2: Efficiency comparison under different conditions in the 12th day.

The 12th day		Input energy (MJ)	Output energy (MJ)	Energy loss (MJ)	Efficiency
Intact rock	Mass control	189.10	183.01	6.09	96.78%
	Air supplement control	195.25	183.48	11.77	93.97%
Rock with single crack	Mass control	189.10	182.46	6.64	96.49%
	Air supplement control	195.25	183.28	11.97	93.87%

Table 3: Efficiency comparison under different conditions in the 20th day.

The 20th day		Input energy (MJ)	Output energy (MJ)	Energy loss (MJ)	Efficiency
Intact rock	Mass control	189.10	182.65	6.45	96.59%
	Air supplement control	195.25	183.26	11.99	93.86%
Rock with single crack	Mass control	189.10	180.31	8.79	95.35%
	Air supplement control	195.25	182.96	12.29	93.71%

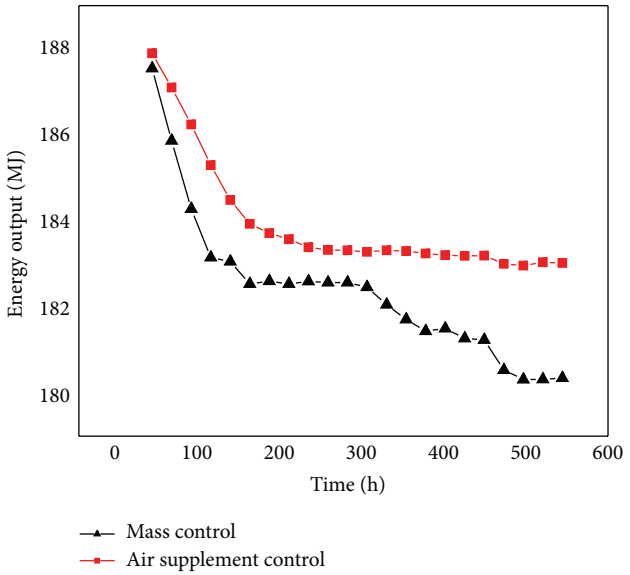

Figure 4: Energy output in rock with single crack.

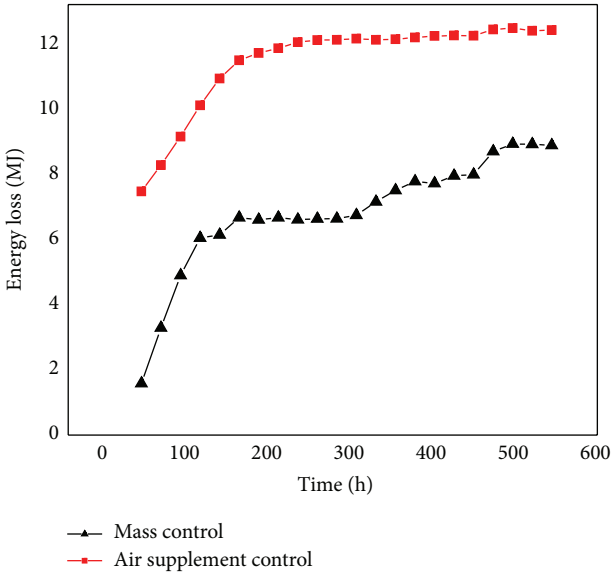

Figure 5: Energy loss in rock with single crack.

air supplement control in the 20th day. The existence of cracks increased the energy loss and the efficiency with mass control is higher than that with air supplement control. However, compared to the 12th day, the efficiency in the 20th day with mass control declined obviously, from 96.49% to 95.35% in rock with single crack. It can be speculated that the air supplement control costs more than mass control but it could maintain relatively stable output energy.

3.2. Energy Analysis in Rock with Multiple Cracks. To study the temperature and pressure fluctuations and energy loss of the CASE plant in hard rock with multiple cracks, we set the location of cracks as shown in Figure 6. In this section, we calculated the model reaction in two cases, namely, the mass control and air supplement control. At the same time, multiple cracks were divided into connected cracks and disconnected cracks.

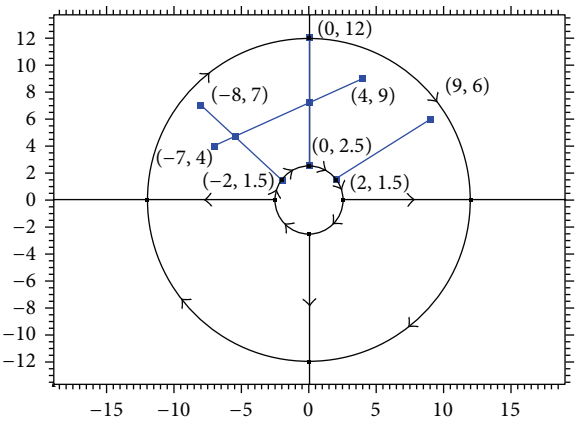

Figure 6: The location of cracks.

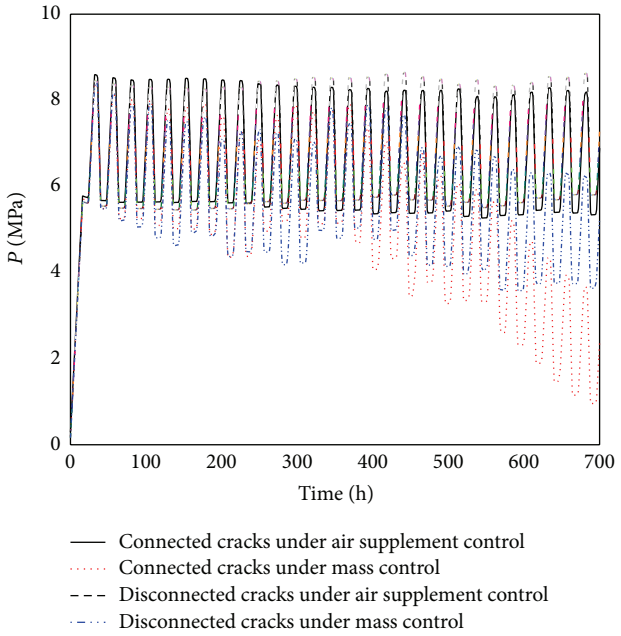

Figure 7: Comparison of pressure between caverns with connected and disconnected cracks.

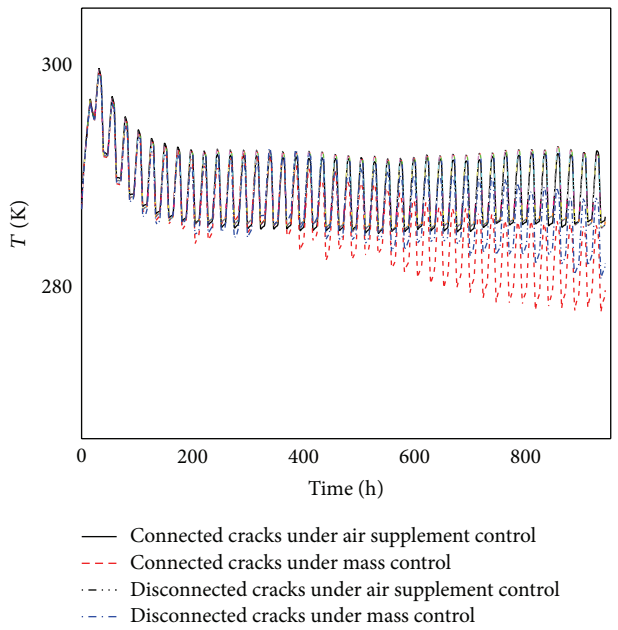

Figure 8: Comparison of temperature between caverns with connected and disconnected cracks.

With air supplement control, the cavern pressure in hard rock with connected and disconnected cracks both fluctuated between 5.5 MPa and 8.5 MPa as shown in Figure 7. In the long term, the cavern pressure with disconnected cracks was higher than that with connected cracks. With mass control, the cavern pressure with disconnected cracks gradually declined while that with connected cracks dropped rapidly, especially after 400 hours of operation. As shown in Figure 8, the temperature of cracked rock cavern with air supplement control fluctuated between 284 K and 292 K while that without additional injection dropped gradually. Connected cracks led to a more significant temperature decrease, which reached 3 degrees at 600 h and 7 degrees at 800 h, while disconnected cracks only resulted in 1 degree loss at 600 h and 3 degrees at 800 h.

As shown in Figure 9, the output energy stayed around 1.84×10^8 J with air supplement control. Without additional air injection, the CASE plant could not maintain stable energy output especially after 400 h. After 800 hours of operation, the energy output of cavern with connected cracks fell to 1.79×10^8 J while that with disconnected cracks only dropped to 1.81×10^8 J. As shown in Figure 10, the energy loss remained around 1.17×10^7 J with supplementary injection. With mass control, the energy loss was 5.6×10^6 J at 200 h but reached 1.01×10^7 J at 800 h with connected cracks and 7.8×10^6 J with disconnected cracks. It can be seen that connected cracks resulted in faster growth of energy loss than disconnected cracks.

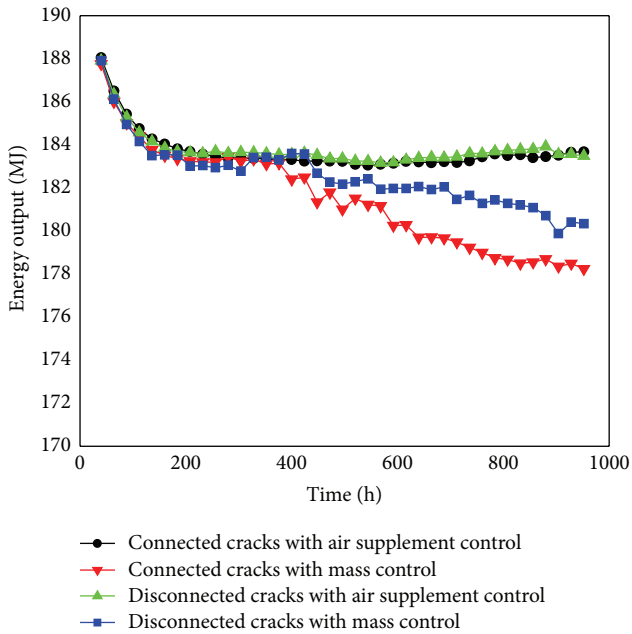

Figure 9: The energy output in caverns with multiple cracks.

4. Sensitivity Analysis of Single Crack

4.1. The Influence of Crack Length. To study the impact of crack length on energy loss, we set the initial crack length as 3.8 m and then increased it by 1.9 m. The crack width is 0.1 m and the location is on the top of carven. As shown in Figure 11, the pressure with air supplement control fluctuated between 5.5 MPa and 8.5 MPa and the change of crack length did not have significant influence on it. Without additional injection, longer crack resulted in faster drop of pressure. It can be seen that crack of 3.8 m in length led to the pressure loss of about 1.5 MPa while 9.5 m resulted in about 3.5 MPa after 500 hours of operation. As shown in Figure 12, without

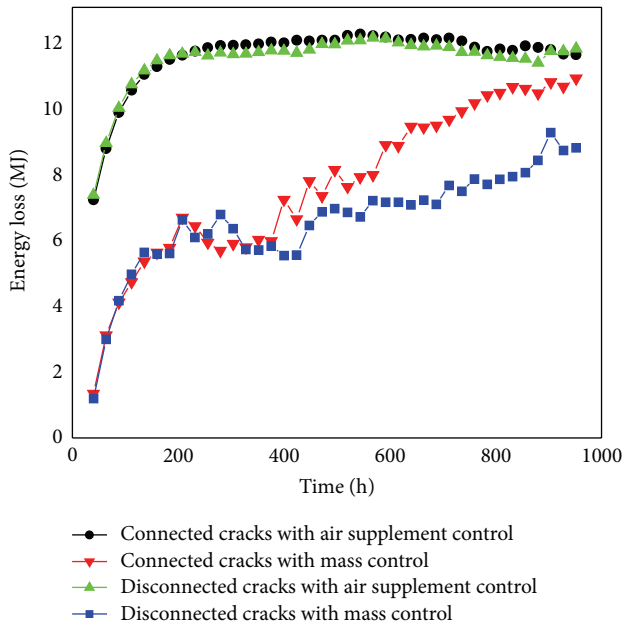

Figure 10: The energy loss in caverns with multiple cracks.

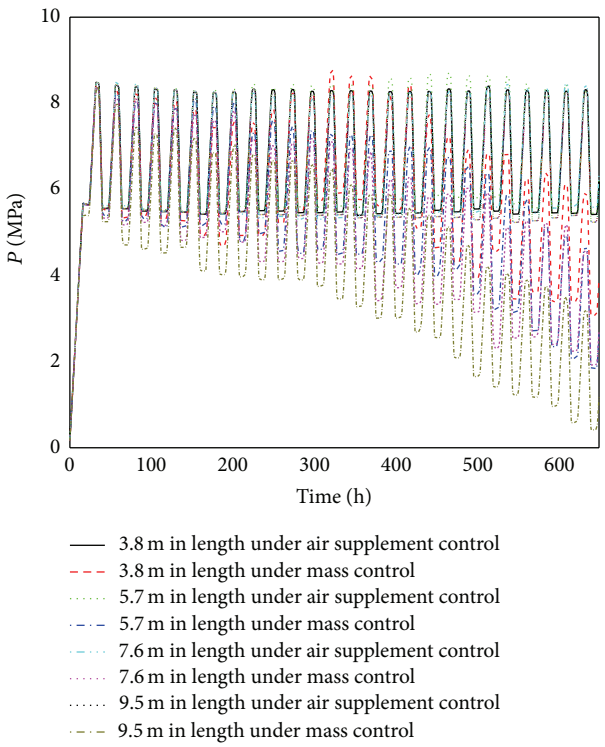

Figure 11: Comparison of pressure between caverns with different length of crack.

supplementary injection, the temperature gradually declined. Longer crack length resulted in more significant decline of temperature. After 600 hours of operation, the cavern with 3.8 m crack has lost about 2.3 degrees of temperature while that with 9.5 m crack was 3.2 degrees.

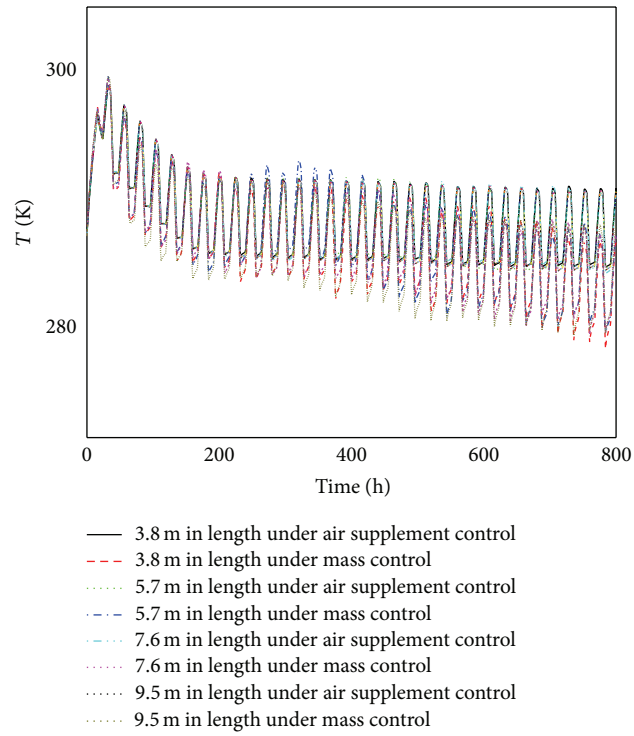

Figure 12: Comparison of temperature between caverns with different length of crack.

It can be seen in Figures 13 and 14 that the length of crack had little influence on the output energy and energy loss with additional air injection which maintained about 1.83×10^8 J and 1.2×10^7 J, respectively. Without supplementary injection, the output energy dropped and energy loss rose over time. After 600 h of operation, the energy loss of cavern with 3.8 m crack was 7.9×10^6 J while that with 9.5 m was 8.0×10^6 J. It can be speculated that the energy loss is not sensitive to the change of fracture length.

4.2. The Influence of the Crack Open Width. We set three different crack widths, namely, 0.001 m, 0.01 m, and 0.1 m. The crack length is 9.5 m and the location is on the top of carven. With air supplement control, the pressure and temperature remained stable as shown in Figures 15 and 16. Without additional air injection, the temperature and pressure declined obviously due to the existence of crack. It can be seen that the single fracture of 0.1 m in width resulted in the pressure loss of about 4 MPa while that of 0.001 m only led to the pressure loss of about 2 MPa. The temperature in 0.1 m width cracked cavern decreased by 3.22 degrees, which was more than that in 0.001 width cracked cavern (2.65 degrees).

As shown in Figures 17 and 18, the energy output and energy loss can be both kept stable with air supplement control. Without additional air injection, the energy output declined over time and the wider crack led to lower output energy. At the same time, the energy loss increased and the wider crack resulted in higher energy loss. After 600 h of

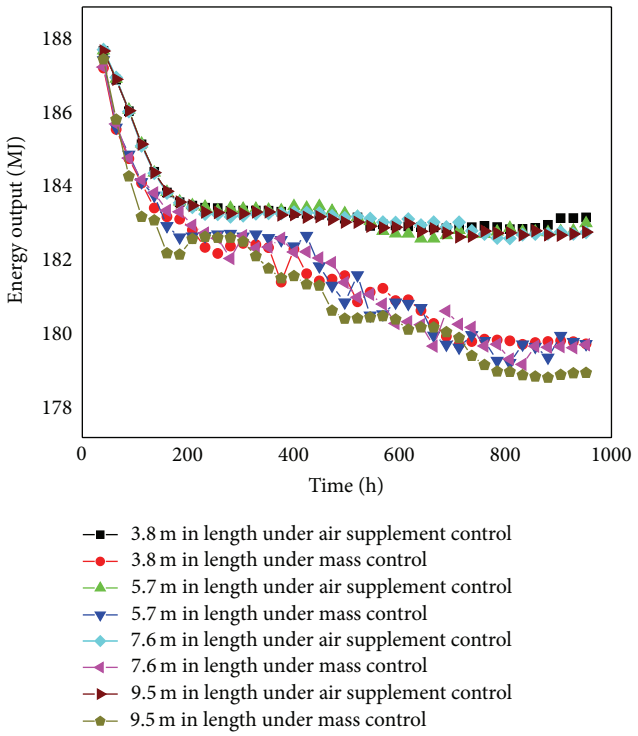

Figure 13: Energy output in caverns with different length of crack.

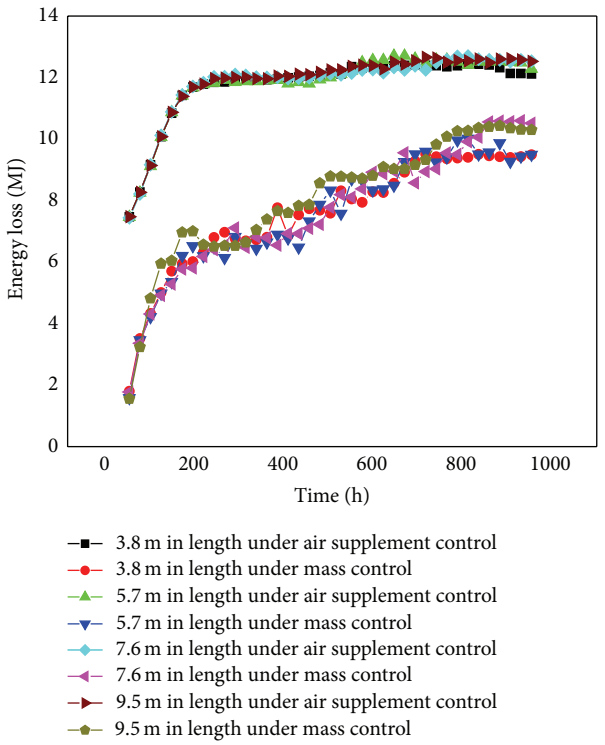

Figure 14: Energy losses in caverns with different length of crack.

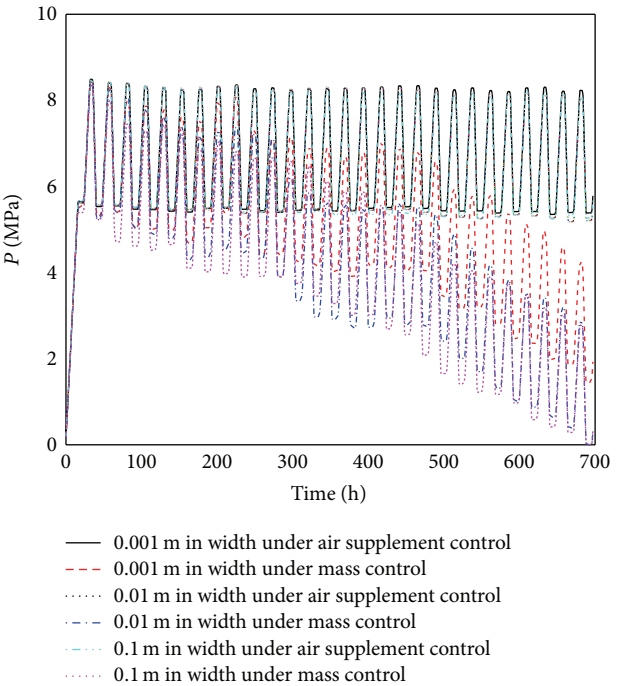

Figure 15: Comparison of pressure between caverns with different width of crack.

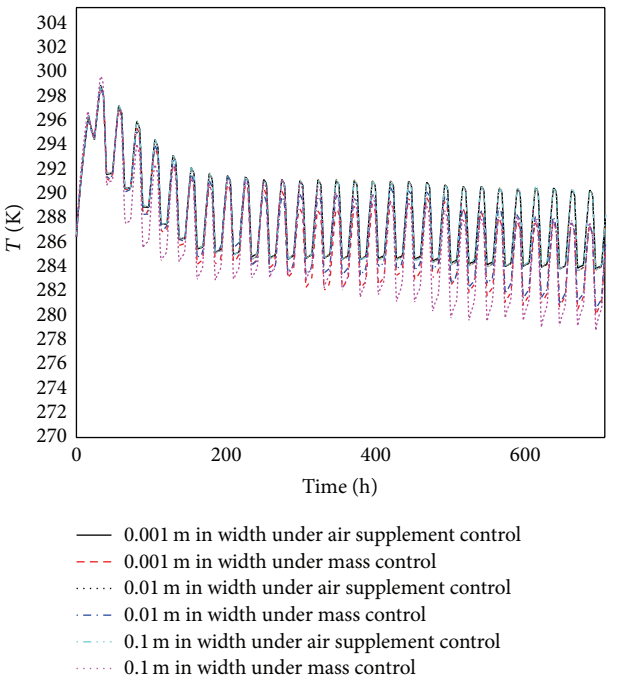

Figure 16: Comparison of temperature between caverns with different width of crack.

operation, the energy loss of cavern with 0.001 m width crack was 6.8×10^6 J while that with 0.1 m was 8.9×10^6 J. It can be speculated that the energy loss is sensitive to the change of fracture open width.

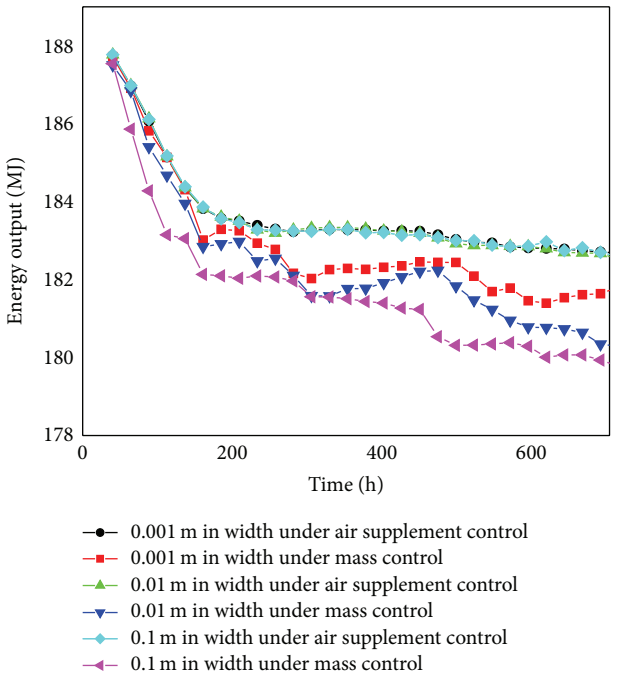

Figure 17: Energy output in caverns with different open width of crack.

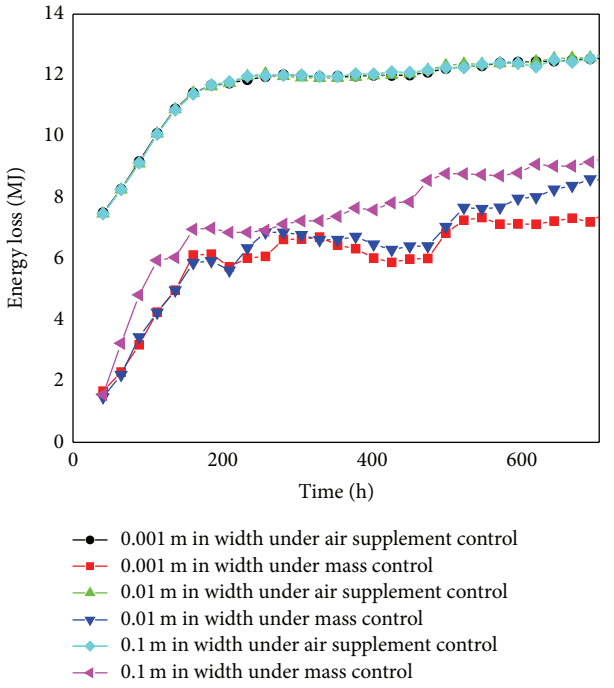

Figure 18: Energy losses in caverns with different open width of crack.

4.3. The Influence of the Crack Position. To study how the crack position influences the energy loss, we place a single crack close to the top of the cavern, at the side and bottom of cavern. The crack width is 0.1 m and the length is 9.5 m. With air supplement control, the pressure fluctuated between 5.5 MPa and 8.5 MPa as shown in Figure 19 and the

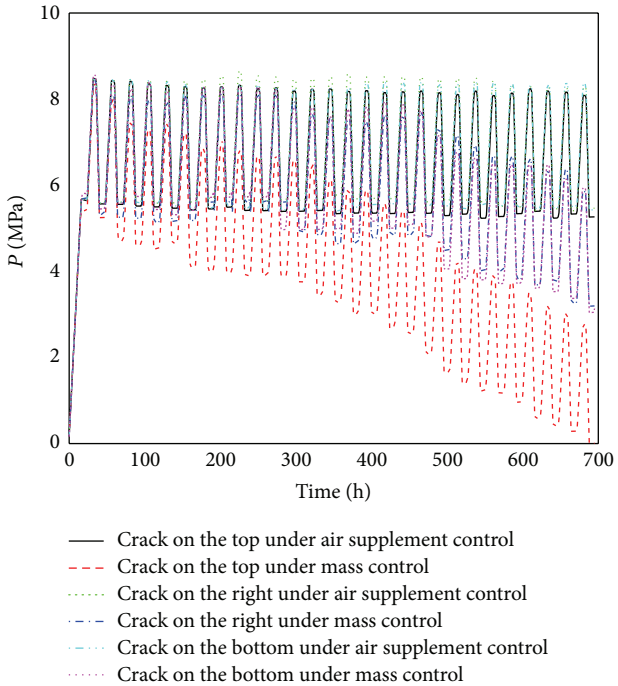

Figure 19: Comparison of pressure between caverns with different location of crack.

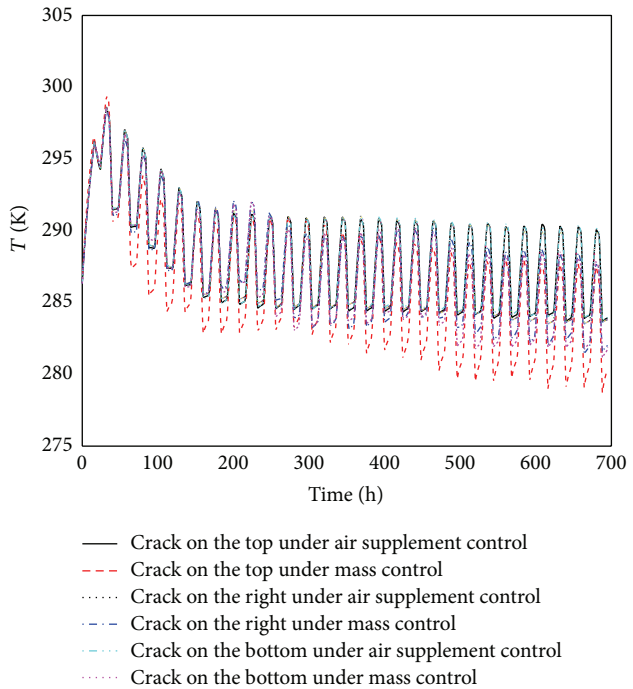

Figure 20: Comparison of temperature between caverns with different location of crack.

temperature fluctuated between 284 K and 294 K as shown in Figure 20. Without additional injection, the pressure and temperature declined gradually. Interestingly, the pressure and temperature in cavern with crack on the top dropped faster than that on the bottom and side.

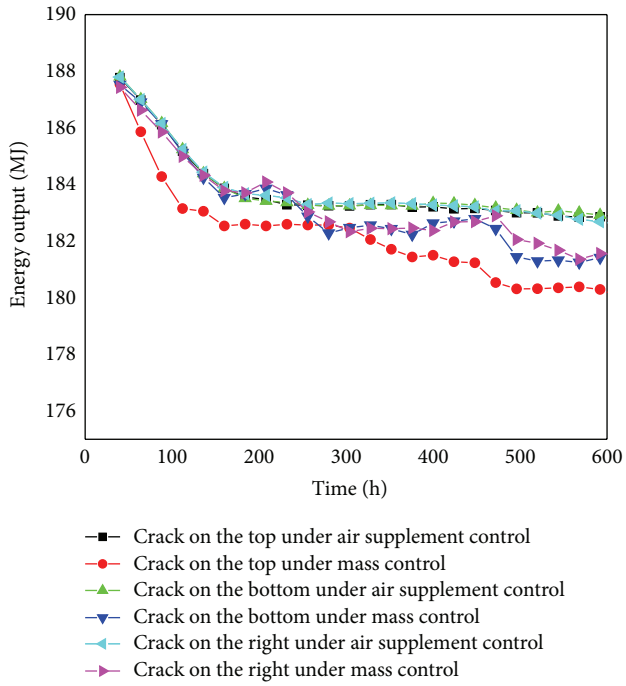

Figure 21: Energy output in caverns with different location of crack.

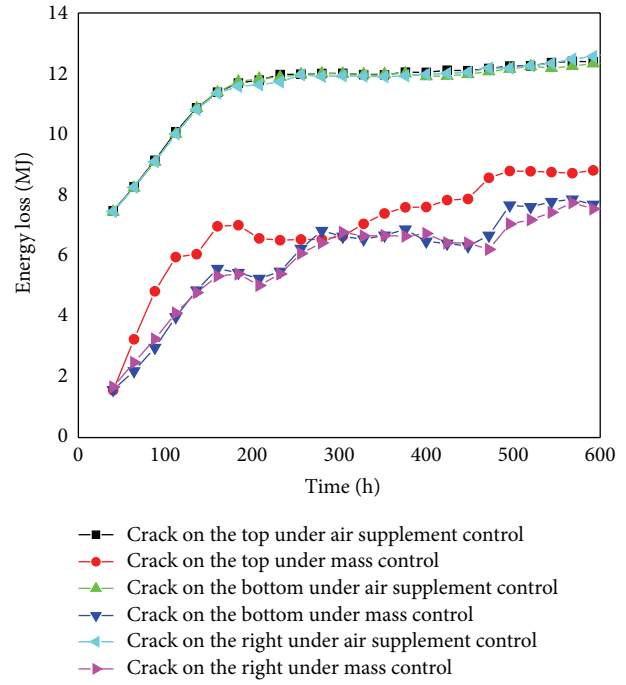

Figure 22: Energy losses in caverns with different location of crack.

As shown in Figures 21 and 22, the energy output and energy loss remained stable with air supplement control. Without additional injection, the energy output of top cracked cavern decreased faster than that of bottom or side cracked cavern. It also can be seen that the energy loss in top cracked cavern had reached 9.09×10^6 J after 600 hours of operation while that in bottom cracked cavern only came to 7.62×10^6 J. The cracks on the top should be paid more attention in the process of CAES plants maintenance.

5. Discussions

In this paper, we conducted the energy analysis of CASE plants built in hard rock. The energy output and energy loss in intact rock and in rock with multiple cracks were studied. We also analyzed the influence of crack length, crack open width, and crack location on the CASE plant operation. It was found that supplementary air injection was an effective way to maintain the normal operation of the CASE plant. Due to the additional injection, the influence of crack on energy output and energy loss was limited. Without supplementary air injection, we found that connected cracks had a greater negative impact on plant operation than disconnected cracks. Furthermore, the output energy and energy loss were sensitive to the change of fracture open width and location. In the process of CAES plants maintenance, we suggest that the cracks on the top should be paid more attention and the open width of cracks should be the key parameter to be monitored. The crack propagation and stress field of rock under different crack conditions are not considered. These can be the topics for further study.

Conflict of Interests

The authors declare that there is no conflict of interests regarding the publication of this paper.

Acknowledgments

The authors would like to acknowledge the support of the present research work from the NSFC (41130751 and 51379147) and the National Basic Research Program of China (973 Program: 2011CB013800) and the support from the Ministry of Science and Technology of China (SLDRCE14-B-31).

References

[1] V. de Biasi, "New solutions for energy storage and smart grid load management," *Gas Turbine World*, vol. 39, pp. 22–26, 2009.

[2] I. Hadjipaschalis, A. Poullikkas, and V. Efthimiou, "Overview of current and future energy storage technologies for electric power applications," *Renewable and Sustainable Energy Reviews*, vol. 13, no. 6-7, pp. 1513–1522, 2009.

[3] C. Pasten and J. C. Santamarina, "Energy geo-storage: analysis and geomechanical implications," *KSCE Journal of Civil Engineering*, vol. 15, no. 4, pp. 655–667, 2011.

[4] H.-M. Kim, J. Rutqvist, D.-W. Ryu, B.-H. Choi, C. Sunwoo, and W.-K. Song, "Exploring the concept of compressed air energy storage (CAES) in lined rock caverns at shallow depth: a modeling study of air tightness and energy balance," *Applied Energy*, vol. 92, pp. 653–667, 2012.

[5] F. Crotogino, K. U. Mohmeyer, and R. Scharf, "Huntorf CAES: more than 20 years of successful operation," in *Proceedings of the Spring SMRI Conference*, Orlando, Fla, USA, 2001.

[6] K. L. DeVries, K. D. Mellegard, G. D. Callahan et al., "Cavern roof stability for natural gas storage in bedded salt," Topical Report Contract DE-FG26-02NT41651, United States Department of Energy and National Energy Technology Laboratory, 2005.

[7] S. Succar and R. H. Williams, "Compressed air energy storage: theory, resources and applications for wind power," Princeton Environmental Institution Report, Compressed Air Energy Storage:Theory,Resources and Applications for Wind Power. Princeton Environmental Institution, 2008.

[8] S. Freiboth, H. Class, R. Helmig et al., "A model for multiphase flow and transport in porous media including a phenomenological approach to account for deformation—a model concept and its validation within a code intercomparison study," *Computational Geosciences*, vol. 13, no. 3, pp. 281–300, 2009.

[9] J. Rutqvist, L. Börgesson, M. Chijimatsu et al., "Thermohydromechanics of partially saturated geological media: governing equations and formulation of four finite element models," *International Journal of Rock Mechanics & Mining Sciences*, vol. 38, no. 1, pp. 105–127, 2001.

[10] T. Rabczuk and T. Belytschko, "A three-dimensional large deformation meshfree method for arbitrary evolving cracks," *Computer Methods in Applied Mechanics and Engineering*, vol. 196, no. 29-30, pp. 2777–2799, 2007.

[11] X. Zhuang, H. Zhu, and C. Augarde, "An improved meshless Shepard and least squares method possessing the delta property and requiring no singular weight function," *Computational Mechanics*, vol. 53, no. 2, pp. 343–357, 2014.

[12] N. Vu-Bac, H. Nguyen-Xuan, L. Chen et al., "A phantom-node method with edge-based strain smoothing for linear elastic fracture mechanics," *Journal of Applied Mathematics*, vol. 2013, Article ID 978026, 12 pages, 2013.

[13] P. Areias and T. Rabczuk, "Finite strain fracture of plates and shells with configurational forces and edge rotations," *International Journal for Numerical Methods in Engineering*, vol. 94, no. 12, pp. 1099–1122, 2013.

[14] Y. Jia, Y. Zhang, G. Xu, X. Zhuang, and T. Rabczuk, "Reproducing kernel triangular B-spline-based FEM for solving PDEs," *Computer Methods in Applied Mechanics & Engineering*, vol. 267, pp. 342–358, 2013.

[15] N. Nguyen-Thanh, N. Valizadeh, M. N. Nguyen et al., "An extended isogeometric thin shell analysis based on Kirchhoff-Love theory," *Computer Methods in Applied Mechanics and Engineering*, vol. 284, pp. 265–291, 2015.

[16] W. Zheng, X. Zhuang, D. D. Tannant, Y. Cai, and S. Nunoo, "Unified continuum/discontinuum modeling framework for slope stability assessment," *Engineering Geology*, vol. 179, pp. 90–101, 2014.

[17] Y. Cai, H. Zhu, and X. Zhuang, "A continuous/discontinuous deformation analysis (CDDA) method based on deformable blocks for fracture modeling," *Frontiers of Structural & Civil Engineering*, vol. 7, no. 4, pp. 369–378, 2013.

[18] J. Frey, R. Chambon, and C. Dascalu, "A two-scale poromechanical model for cohesive rocks," *Acta Geotechnica*, vol. 8, no. 2, pp. 107–124, 2013.

[19] X. Zhuang, Q. Wang, and H. Zhu, "A 3D computational homogenization model for porous material and parameters identification," *Computational Materials Science*, vol. 96, pp. 536–548, 2015.

[20] T. Rabczuk and T. Belytschko, "Cracking particles: a simplified meshfree method for arbitrary evolving cracks," *International Journal for Numerical Methods in Engineering*, vol. 61, no. 13, pp. 2316–2343, 2004.

[21] T. Rabczuk and T. Belytschko, "A three-dimensional large deformation meshfree method for arbitrary evolving cracks," *Computer Methods in Applied Mechanics and Engineering*, vol. 196, no. 29-30, pp. 2777–2799, 2007.

[22] P. R. Budarapu, R. Gracie, S.-W. Yang, X. Zhuang, and T. Rabczuk, "Efficient coarse graining in multiscale modeling of fracture," *Theoretical and Applied Fracture Mechanics*, vol. 69, pp. 126–143, 2014.

[23] P. R. Budarapu, R. Gracie, S. P. A. Bordas, and T. Rabczuk, "An adaptive multiscale method for quasi-static crack growth," *Computational Mechanics*, vol. 53, no. 6, pp. 1129–1148, 2014.

[24] H. Talebi, M. Silani, and T. Rabczuk, "Concurrent multiscale modeling of three dimensional crack and dislocation propagation," *Advances in Engineering Software*, vol. 80, pp. 82–92, 2015.

[25] H. Talebi, M. Silani, S. P. A. Bordas, P. Kerfriden, and T. Rabczuk, "Molecular dynamics/xfem coupling by a three-dimensional extended bridging domain with applications to dynamic brittle fracture," *International Journal for Multiscale Computational Engineering*, vol. 11, no. 6, pp. 527–541, 2013.

[26] J. Noorishad, C. F. Tsang, and P. A. Witherspoon, "Coupled thermal-hydraulic-mechanical phenomena in saturated fractured porous rocks: numerical approac," *Journal of Geophysical Research*, vol. 89, no. 12, pp. 10365–10373, 1984.

[27] R. W. Zimmerman, "Coupling in poroelasticity and thermoelasticity," *International Journal of Rock Mechanics and Mining Sciences*, vol. 37, no. 1-2, pp. 79–87, 2000.

[28] W. Obeid, G. Mounajed, and A. Alliche, "Mathematical formulation of thermo-hygro-mechanical coupling problem in non-saturated porous media," *Computer Methods in Applied Mechanics and Engineering*, vol. 190, no. 39, pp. 5105–5122, 2001.

[29] J. Rutqvist, L. Börgesson, M. Chijimatsu et al., "Thermohydromechanics of partially saturated geological media: governing equations and formulation of four finite element models," *International Journal of Rock Mechanics and Mining Sciences*, vol. 38, no. 1, pp. 105–127, 2001.

[30] J. Rutqvist, Y.-S. Wu, C.-F. Tsang, and G. Bodvarsson, "A modeling approach for analysis of coupled multiphase fluid flow, heat transfer, and deformation in fractured porous rock," *International Journal of Rock Mechanics and Mining Sciences*, vol. 39, no. 4, pp. 429–442, 2002.

[31] M. Raju and S. Kumar Khaitan, "Modelling and simulation of compressed air storage in caverns: a case study of the Huntorf plant," *Applied Energy*, vol. 89, no. 1, pp. 474–481, 2012.

[32] R. Kushnir, A. Dayan, and A. Ullmann, "Temperature and pressure variations within compressed air energy storage caverns," *International Journal of Heat and Mass Transfer*, vol. 55, no. 21-22, pp. 5616–5630, 2012.

[33] X. Zhuang, R. Huang, C. Liang, and T. Rabczuk, "A coupled thermo-hydro-mechanical model of jointed hard rock for compressed air energy storage," *Mathematical Problems in Engineering*, vol. 2014, Article ID 179169, 11 pages, 2014.